Structural and functional analysis of the C-terminal STAS domain of the Arabidopsis thaliana sulfate transporter SULTR1.2

H. Rouached, P. Berthomieu, E. El Kassis, N. Cathala, V. Catherinot, G. Labesse, J.C. Davidian, P. Fourcroy

THE JOURNAL OF BIOLOGICAL CHEMISTRY
Vol. 280, No. 16, Issue of April 22, pp. 15976–15983, 2005

Printed in U.S.A.

Structural and Functional Analysis of the C-terminal STAS (Sulfate Transporter and Anti-sigma Antagonist) Domain of the *Arabidopsis thaliana* Sulfate Transporter SULTR1.2*

Received for publication, February 11, 2005
Published, JBC Papers in Press, February 16, 2005, DOI 10.1074/jbc.M501635200

Hatem Rouached‡, Pierre Berthomieu‡, Elie El Kassis‡, Nicole Cathala‡, Vincent Catherinot§, Gilles Labesse§, Jean-Claude Davidian‡, and Pierre Fourcroy‡¶

From the ‡Biochimie et Physiologie Moléculaire des Plantes, CNRS (UMR 5004), Université Montpellier 2, Institut National de la Recherche Agronomique, Ecole Nationale Supérieure Agronomique, Montpellier, 34060 France and §Centre de Biochimie Structurale, INSERM U554, Centre National de la Recherche Scientifique (UMR 5048), Université Montpellier I, Montpellier, 34060 France

The C-terminal region of sulfate transporters from plants and animals belonging to the SLC26 family members shares a weak but significant similarity with the *Bacillus* sp. anti-anti-sigma protein SpoIIAA, thus defining the STAS domain (sulfate transporter and anti-sigma antagonist). The present study is a structure/function analysis of the STAS domain of SULTR1.2, an *Arabidopsis thaliana* sulfate transporter. A three-dimensional model of the SULTR1.2 STAS domain was built which indicated that it shares the SpoIIAA folds. Moreover, the phosphorylation site, which is necessary for SpoIIAA activity, is conserved in the SULTR1.2 STAS domain. The model was used to direct mutagenesis studies using a yeast mutant defective for sulfate transport. Truncation of the whole SULTR1.2 STAS domain resulted in the loss of sulfate transport function. Analyses of small deletions and mutations showed that the C-terminal tail of the SULTR1.2 STAS domain and particularly two cysteine residues plays an important role in sulfate transport by SULTR1.2. All the substitutions made at the putative phosphorylation site Thr-587 led to a complete loss of the sulfate transport function of SULTR1.2. The reduction or suppression of sulfate transport of the SULTR1.2 mutants in yeast was not due to an incorrect targeting to the plasma membrane. Both our three-dimensional modeling and mutational analyses strengthen the hypothesis that the SULTR1.2 STAS domain is involved in protein-protein interactions that could control sulfate transport.

Sulfur (S) is an essential macro-nutrient for microorganism, animal, and plant growth. In plants sulfate is the main sulfur source acquired from the soil solution. After being absorbed through the plasma membrane of epidermis and cortical root cells, sulfate is transported within the plant through numerous cell membranes under the control of a surfeit of sulfate transporters (1). The variety of locations and sensitivities to sulfate availability of the latter contribute to the plant sulfur homeostasis. Animal cells also transport sulfate through their membranes, and in mammals some diseases or developmental abnormalities were shown to be caused by defective sulfate transports (2). For example, mutations of the diastrophic dysplasia gene induce deficient intracellular sulfate pools in chondrocytes, leading to the production of undersulfated proteoglycans, which impair the synthesis of cartilage (3).

Sulfate transport in plants has been shown to be a H^+-dependent co-transport process (4–6). In contrast, animal sulfate transport systems are described and characterized as being either Na^+-dependent or Na^+-independent transporters (7). When Na^+ is not required, as for transporters belonging to the SLC4 and SLC26 families, sulfate uptake is mediated by a sulfate-anion antiporter system using bicarbonate, chloride, organic acids, or esterified bile acids as the counter-anion. The protein structure of the animal Na^+-independent sulfate transporters is quite similar to that of the plant sulfate transporters. These transporters generally have 9–11 predicted membrane-spanning helixes and possess a long hydrophilic region downstream the last transmembrane helix. This C-terminal region shows an unexpected sequence similarity with a family of bacterial proteins called SpoIIAA and known as anti-sigma factor antagonists. Because of this sequence similarity, the C-terminal region of the sulfate transporters has been defined as a STAS[1] domain (for sulfate transporters anti-sigma antagonist domain) (8). The bacterial SpoIIAA protein is a key component of the regulation network involved in the induction of sporulation in response to nutrient deficiency (9, 10). In normal growing conditions, SpoIIAA is phosphorylated on its serine 58, and SpoIIAB is complexed with a sporulation-inducing sigma factor, which is thus inactive. Under nutrient deficiency SpoIIE, a specific phosphatase for SpoIIAA phosphate, becomes active; the dephosphorylation of SpoIIAA allows it to interact with SpoIIAB. As a result, the sigma factor is released from SpoIIAB and induces sporulation (9, 11).

The functional role of the STAS domain with respect to sulfate transport is completely unknown. Up to now structure-function studies of plant and animal sulfate transporters have mainly focused on the transmembrane domain regions (12, 13). However, in animal cells it has been recently reported that the STAS domain of the human chloride-bicarbonate exchanger DRA is involved in protein-protein interaction with the cystic fibrosis transmembrane conductance regulator (CFTR), thus

* This work was supported by grants from the French research organizations Institut National de la Recherche Agronomique and CNRS and fellowships from the French Ministère de l'Enseignement Supérieur et de la Recherche (to E. E. K.) and from the Tunisian government (to H. R.). The costs of publication of this article were defrayed in part by the payment of page charges. This article must therefore be hereby marked "*advertisement*" in accordance with 18 U.S.C. Section 1734 solely to indicate this fact.

¶ To whom correspondence should be addressed. Tel.: 33-499-612-612; Fax: 33-467-525-737; E-mail: fourcroy@ensam.inra.fr.

[1] The abbreviations used are: STAS, sulfate transporter and anti-sigma antagonist; DRA, down-regulated in adenoma; MES, 2-(*N*-morpholino)ethanesulfonic acid; Bis-Tris, bis(2-hydroxyethyl)iminotris(hydroxymethyl)methane.

resulting in the mutual activation of both DRA and CFTR (14). This result suggests that the STAS domain of transporters from eukaryotes may play a regulatory role through protein-protein interactions, as SpoIIAA does in *Bacillus subtilis*.

Recently, a study demonstrated the importance of the STAS domain as a whole for the function of *Arabidopsis thaliana* sulfate transporters and showed that the STAS domain is not interchangeable between 3 of the 12 *A. thaliana* sulfate transporters that possess a STAS domain (15). We performed a structure-function analysis of the STAS domain of the *Arabidopsis* high affinity sulfate transporter SULTR1.2, which is believed to be responsible for ~70% of sulfate uptake by roots (16, 17). We first propose a three-dimensional modeling of the SULTR1.2 STAS domain that highlights its structural similarity with the well characterized SpoIIAA protein structure, particularly at the putative phosphorylation site. Then, using a yeast mutant defective in its sulfate transport capacity as a functional expression system, we identified by serial deletions and mutagenesis some key amino acids of the STAS domain that are essential for the sulfate transport function of SULTR1.2.

EXPERIMENTAL PROCEDURES

Computational Sequence Analysis—Structural predictions, fold recognition, and sequence threading onto three-dimensional structures were carried out using 3D-PSSM, FUGUE, and GenTHREADER through the @TOME meta-server available at bioserv.cbs.cnrs.fr (18). TITO (Tool for Incremental Threading Optimization) was applied automatically to evaluate the sequence-structure alignment provided by the meta-server. Edition and optimization of the alignment was performed using the program ViTO.[2] Promising sequence-structure alignments were further submitted to MODELLER 6.2 for comparative protein modeling by satisfaction of spatial restraints (19). Resulting models were evaluated using the programs Verify3D (20) and PROSA (21).

Plasmid Constructions and Site-directed Mutagenesis—All the constructs were performed by PCR amplification with the high fidelity *Pfu* DNA polymerase (Promega, Madison, WI) using the *Arabidopsis* full-length *SULTR1.2* cDNA as template. The amplification products corresponding to the wild-type SULTR1.2 transporter, to the mutant SULTR1.2 transporters harboring deletions of the last 4, 7, 8, 12, or 131 amino acids, or to the mutant SULTR1.2 transporters harboring the simple C645S, C646S, or double C645S/C646S substitutions were obtained using the same forward primer, 5′-ATgTCgTCAAgAgCTCACCCTgTggAC-3′, and the following reverse primers, 5′-TCAgACCTCgTTggAgAgTTTTggACAg-3′, 5′-TCATCAgAgTTTTggACAgCAAgCCTCgACg-3′, 5′-CTATCAACAgCAAgCCTCgACggCATCA-3′, 5′-TCATCAgCAAgCCTCgACggCATCAgCCACCg-3′, 5′-CTACTAggCATCAgCCACCgTTAgATAgAT-3′, 5′-TCATCACTgTTgAATATTTCTgTAAAC-3′, 5′-TCAgACCTCgTTggAgAgTTTTggAgAgCAAgCC-3′, 5′-TCAgACCTCgTTggAgAgTTTTggACAggAAgCC-3′, and 5′-TCAgACCTCgTTggAgAgTTTTggAgAggAAgCC-3′, respectively. The PCR products were cloned into the pCR-Script SK+ vector (Stratagene, La Jolla, CA) at the SrfI restriction site in the appropriate orientation.

The site-directed mutageneses corresponding to the deletion of threonine 587 (T587ΔT) and to the T587S, T587A, or T587D substitutions were performed in two steps. In the first step and for every mutagenesis experiment, two PCR products were generated using the full-length *SULTR1.2* cDNA as template; one of the PCR constructs consisted of the beginning of the *SULTR1.2* coding sequence, from the start codon to the mutagenized threonine 587 codon, and the other consisted of the end of the *SULTR1.2* coding sequence, from the mutagenized threonine 587 codon to the stop codon. Both PCR products were separately cloned in the pCR-Script SK+ vector at the SrfI restriction site and in the appropriate orientation. In the second step the whole mutagenized coding sequence was reassembled by in-frame subcloning of the 3′ end of the coding sequence downstream of the 5′ end. For every site-directed mutagenesis, this two-step cloning procedure required the use of appropriate PCR primers, which harbored the desired mutation of the threonine 587 codon and which were partially overlapping and contained a common restriction site enabling the in-frame assembly of the whole coding sequence. For the different site-directed mutageneses, the 5′-gCTCCggAATCgATgTCCgTAACAggTgAC-3′ (T587ΔT-rev), 5′-ACgTCTAgAATCgATgTCCgTAACAggTgA-3′ (T587S-rev), 5′-CTAgCTAgCATCgATgTCCgTAACAggTgA-3′ (T587A-rev), 5′-gCTCCggAgTCATCgATgTCCgTAACAggT-3′ (T587D-rev), reverse primers were used in combination with the forward 5′-ATgTCgTCAAgAgCTCACCCTgTggAC-3′ primer to amplify the beginning of the *SULTR1.2* coding sequence. The 5′-gCTCCggAATTCACgCATTAgAAgACTTAT-3′ (T587ΔT-fw), 5′-TTAgCTAgCggTATTCACgCATTAgAAgAC-3′ (T587S-fw), 5′-TTAgCTAgCggTATTCACgCATTAgAAgAC-3′ (T587A-fw), or 5′-gCTCCggAATTCACgCATTAgAAgACTTAT-3′ (T587D-fw) forward primers were used in combination with the 5′-TCAgACCTCgTTgtgAgAgTTTTggACAg-3′ reverse primer to amplify the end of the *SULTR1.2* coding sequence. The restriction sites used for the reassembly of the whole coding sequence corresponding to the deletion of threonine 587 and to the T587S, T587A, or T587D substitutions were BseA1, XbaI/NheI, NheI, and BseA1, respectively (underlined in the primer sequences).

The DNA sequences of the constructs were checked (GenomeExpress, Grenoble, France). Then, for every construct a HindIII-NotI fragment comprising the whole coding sequence was subcloned at the corresponding sites into the yeast expression vector pYES2 (Invitrogen) under the control of the inducible *GALI* promoter.

Construction of Wild-type and Mutant SULTR1.2::FLAG Protein Fusions—In a first step the wild-type coding sequence of *SULTR1.2* was fused at its 3′ end to the DNA sequence encoding the FLAG® epitope tag DYKDDDDK in the yeast expression vector pESC-URA (Stratagene). For that, PCR amplification was performed with the high fidelity *Pfu* DNA Polymerase (Promega) using the *Arabidopsis* full-length *SULTR1.2* cDNA as template and the forward 5′-AtgTCgTCAAgAgCTCACCCTgTggAC-3′ and reverse 5′-CCTggACTAgTCCgACCTCgTTggAggAgTTTTgg-3′ primers. The latter primer was designed so that it enabled the replacement of the *SULTR1.2* stop codon by a new SpeI restriction site (underlined in the primer sequence) allowing in-frame fusion with the FLAG® sequence. The PCR product was cloned into the pCR-Script SK+ vector (Stratagene) at the SrfI site and in the appropriate orientation. The EcoRI-SpeI fragment comprising the whole *SULTR1.2* coding sequence was then subcloned into pESC-URA at the EcoRI/SpeI sites, giving the pESC-*SULTR1·2*::*FLAG* vector. The *SULTR1.2*::*FLAG* fusion was under the control of the inducible yeast *GAL10* promoter.

The mutant *SULTR1.2*::*FLAG* fusions were constructed in a second step. The mutant *SULTR1.2* clones described above were used as template for PCR amplification using the high fidelity *Pfu* DNA Polymerase (Promega). Only the STAS region of the mutant *SULTR1.2* was amplified. The forward 5′-CCAAgAACTTCggTTTACAgAAATATTC-3′ primer was used in combination with the reverse 5′-CCTggACTAgTCCgACCTCgTTggAgAgTTTTgg-3′ primer for all the constructs except for the SULTR1.2 Δ12 construct for which the reverse primer was 5′-CCggACTAgTCCggCATCAgCCACCgTTAgATA-3′. The PCR products were digested with both the AvrII and SpeI restriction enzymes, and the resulting fragments were introduced in pESC-URA *SULTR1.2*::*FLAG* at the corresponding sites, replacing the wild-type fragment by the mutated ones. All the constructions were verified by sequencing.

Yeast Transformation and Growth—The pYES2 plasmids harboring the wild-type and mutant SULTR1.2 transporters were introduced in the *Saccharomyces cerevisiae* strain YSD1 (MATα, *his3*, *leu2*, *ura3*, *sul1*) (22), which is unable to grow when sulfate is the sole sulfur source in the medium but grows on medium supplied with a reduced sulfur source such as homocysteine. Genetic transformation was performed using the S.c. Easy Comp™ system (Invitrogen). YSD1 transformed with the empty expression vector pYES2 was used as a negative control. Recombinant yeast cells were grown for at least 6 generations to ~1 $A_{600\ nm}$ unit in a rich but uracil-free medium containing 0.7% (w/v) yeast nitrogen base (Difco), 0.1% (w/v) casamino acids (Difco), 5% (w/v) glucose, 0.75 mM leucine, and 1 mM histidine. Yeast cells were then washed once with sterile deionized water and resuspended to a final absorbance of 1 $A_{600\ nm}$ unit in a selective synthetic minimal medium called B medium containing 15 mM NH_4Cl, 6.6 mM KH_2PO_4, 0.5 mM K_2HPO_4, 2 mM $MgCl_2$, 1.7 mM NaCl, 0.68 mM $CaCl_2$, 80 μM H_3BO_3, 6 μM KI, 4 μM $ZnCl_2$, 2 μM $CuCl_2$, 1.8 μM $FeCl_3$, 1% (w/v) galactose, 0.75 mM leucine, and 1 mM histidine (23). For the drop tests 30 μl of the final suspension and of 10 and 100 times dilutions of the final suspension were dropped on the selective synthetic B medium containing either 0.1 mM Na_2SO_4 or 0.1 mM homocysteine as the sole sources of sulfur solidified with 1% (w/v) low sulfate containing agarose (Invitrogen). Yeast cells were grown for 3 days at 30 °C. For growth analyses in liquid cultures, YSD1 cells expressing the various pYES2::SULTR1.2 constructs were grown in synthetic selective B medium containing 0.1 mM Na_2SO_4 under vigorous shaking (200 rpm) at 30 °C. The doubling times

[2] V. Catherinot and G. Labesse, unpublished results.

were calculated from linear regression of the $\log_2$ values of the A_{600} per time in the exponential phase growth.

Sulfate Uptake Assays—Sulfate uptake assays were performed as already described (24) with the following modifications. For the sulfate influx measurement, yeast cells were rinsed and resuspended in a sulfate-free solution (1% (w/v) galactose, 0.1 mM homocysteine, 0.75 mM leucine, and 1 mM histidine), the pH of which was adjusted to 5.0 by the addition of MES. Every sulfate uptake measurement was started by adding simultaneously K_2SO_4 at the final concentration of 0.1 mM and 3.7×10^4 Bq of [^{35}S]sulfate (Amersham Biosciences).

Protein Extraction and Analysis—Yeast cells were grown up to 0.2–0.4 A_{600} unit in synthetic selective B medium supplemented with 0.1 mM homocysteine, washed once in cold TE buffer (10 mM Tris HCl, pH 7.6, 1 mM EDTA), and resuspended in cold extraction buffer containing 50 mM Bis-Tris propane, pH 7.6, 0.3 M mannitol, 5 mM Na_2EDTA, 5 mM $MgCl_2$, 1 mM dithiothreitol, 1 mM phenylmethylsulfonyl fluoride, and 0.2% (v/v) of a yeast protease inhibitor mixture (Sigma). Yeast cells were disrupted at 120 megapascals at 4 °C using the Z PLUS 1.1 KW Benchtop Cell Disrupter (Constant Systems, Warwick, UK). The homogenate was clarified by centrifugation at 2000 × *g* for 5 min at 4 °C, and the resulting supernatant was centrifuged at 80,000 × *g* for 1 h at 4 °C. The soluble proteins present in the supernatant were precipitated in 10% (w/v) trichloroacetic acid, kept on ice overnight, pelleted at 45,000 × *g* for 30 min at 4 °C, and resuspended in a storage TE buffer containing 1 mM dithiothreitol and 0.2% (v/v) of the yeast protease inhibitor mixture. The 80,000 × *g* pellet containing the crude membrane fraction was resuspended in cold storage TE buffer containing 10% (w/w) sucrose and deposited on a discontinuous 25–37-53% (w/w) sucrose gradient prepared in a TE buffer. After centrifugation in the SW41Ti rotor (Beckman Coulter, Fullerton, CA) at 150,000 × *g* for 19 h at 4 °C, the plasma membrane-enriched fraction corresponding to the 37–53% interface (25) was collected, diluted 10 times in cold storage buffer, pelleted at 80,000 × *g* for 1 h at 4 °C, and resuspended in cold storage buffer. Protein concentrations were determined according to the Schaffner procedure (26) using bovine serum albumin as a standard. For electrophoresis, 10 μg of proteins were mixed with ⅓ volume of 4× loading buffer (200 mM Tris-HCl, pH 6.5, 8% (w/v) SDS, 8% (v/v) β-mercaptoethanol, 40% (v/v) glycerol, and 0.04% (w/v) bromophenol blue) and heated at 37 °C for 20 min. Protein samples were resolved on a 12% (w/v) polyacrylamide gel by SDS-PAGE and then electrotransferred (100 V, 1 h) onto polyvinylidene difluoride Immobilon-P membranes (Millipore, Bedford, MA). The blotted membrane was treated with methanol 95% (v/v) for 15 s, dried at 37 °C for 15 min, incubated in phosphate-buffered saline buffer containing 0.01% (v/v) Tween, 2% (w/v) bovine serum albumin and the appropriate antibody for 1 h, then washed in phosphate-buffered saline buffer containing 0.01% (v/v) Tween for 30 min. A 1:30,000 dilution of the alkaline phosphatase-conjugated monoclonal anti-FLAG® antibody (Sigma) was used to immuno-detect the SULTR1.2::FLAG fusion proteins. A 1:100,000 dilution of the polyclonal antibody raised against the *Nicotiana plumbaginifolia* H^+-ATPase PMA2 (27) was used to reveal the yeast H^+-ATPase, a marker of the plasma membrane. This antibody was detected by an alkaline phosphatase-conjugated goat anti-Rabbit IgG secondary antibody (Promega). Alkaline phosphatase activity was detected using the CDP Star enhanced chemiluminescence substrate (Roche Applied Science).

RESULTS

Three-dimensional Modeling of the STAS Domain of the Arabidopsis Sulfate Transporter SULTR1.2—The sequences of the C-terminal regions of a set of sulfate transporters from plant, animal, and yeast were compared with the prokaryotic sequences of the anti-anti-sigma factors SpoIIAA of *B. subtilis* (1AUZ) and *Bacillus sphaericus* (1H4Z) (Fig. 1*A*). Significant sequence similarities (35–80% of amino acid identity were found in the C-terminal regions of the plant sulfate transporters (SULTR1.1, SULTR1.2, SULTR2.1, and SULTR2.2 from *Arabidopsis* and ShST1 from *Stylosanthes hamata*). In contrast, the sequence similarities between the plant sulfate transporter C-terminal regions and the human diastrophic dysplasia sulfate transporter, the *S. cerevisiae* sulfate transporter SUL1, or the *Bacillus* anti-anti-sigma factors SpoIIAA were weaker (15–20% of amino acid identity. However, these low sequence similarities occurred at very specific positions (Fig. 1*A*), which had already been shown to define the so-called STAS domain.

We further characterized the *Arabidopsis* sulfate transporter STAS domains at the secondary and tertiary structure levels by comparing these domains with the available NMR structure of *B. subtilis* SpoIIAA (28) and the crystal structure of *B. sphaericus* SpoIIAA (29). The dedicated meta-server @TOME available at bioserv.cbs.cnrs.fr (18) was used for the fold compatibility analyses. With most queries (including those in Fig. 1*A*), mGenTHREADER, 3D-PSSM, and FUGUE showed highly significant threading scores (*e* values of 0.008, $3e-5$, and Z-score of 15.9, respectively) with SpoIIAA structures. The structural analysis was further developed for the SULTR1.2 STAS domain. Various models were built using the programs TITO and MODELLER (19). Assessment of these computed three-dimensional models by molecular structure and amino acid environment evaluation tools such as Verify3D, ERRAT, and PROSA, showed that the models were very good (scoring above 0.3 with Verify3D and above 70% with ERRAT; pseudo-energy was below −1.2 as computed by PROSA). These results validated the structural alignment of the SULTR1.2 STAS domain with the NMR and crystal structures of SpoIIAA, and thus, the resulting three-dimensional model specifically built for SULTR1.2 (Fig. 1).

The structural analysis revealed a compact hydrophobic core at the interface of the α-helices and the β-sheets. This hydrophobic core appeared very well conserved between the SULTR1.2 STAS domains and SpoIIAA (Fig. 1*B*). The structural analysis also revealed that the phosphorylation site, which is critical for SpoIIAA function (9), is conserved in the SULTR1.2 STAS domain and more generally in almost all the other sulfate transporter STAS domains. This phosphorylation site consists of an aspartate (strictly conserved in all the sulfate transporter STAS domains and in SpoIIAA) followed by one or two hydroxyl-containing amino acids and a structurally preferred glycine (motif D(S/T)(2)G) (Fig. 1*A*). Conservation of this phosphorylation site suggests that phosphorylation is a key determinant of SULTR1.2 activity as it is for SpoIIAA.

The major difference between the modeled STAS domain and the SpoIIAA structure lies at the connection between the SULTR1.2 α1-helix and β3-sheet (Fig. 1*A*). At this position all the sulfate transporter STAS domains display variable lengths of amino acid insertions. This variable region lies at the periphery of the domain and is far away from the common phosphorylation region (Fig. 1*B*). The modeled STAS domain also differed from the SpoIIAA structure at the very C terminus. This region is highly variable in length and sequence even between the various sulfate transporters. At the end of the C-terminal α4-helix of its STAS domain, SULTR1.2 possesses a pair of cysteines (Cys-645, Cys-646) that is not strictly conserved in the paralogs and which is not present in SpoIIAA (Fig. 1*A*). The first cysteine (Cys-645) is fairly conserved between the *Arabidopsis* sulfate transporters, and it is substituted by a hydrophobic residue in the other sulfate transporters. The second cysteine (Cys-646) is specific for SULTR1.2, and it is substituted by polar amino acids in the other sulfate transporters. The putative role of these cysteines was analyzed in view of the current three-dimensional model.

In conclusion, the structural analysis and modeling strongly suggest that the SULTR1.2 C-terminal STAS domain shares the SpoIIAA fold, although it shows low overall sequence identity with SpoIIAA (~17% over 130 residues). The structural similarity is particularly high in the vicinity of the phosphorylation site despite the change from a conserved serine in SpoIIAA to the similar amino acid threonine in SULTR1.2.

The STAS Domain Is Necessary for Sulfate Transport by SULTR1.2 in Yeast—The functional importance of the STAS domain for sulfate transport by SULTR1.2 was first checked. A SULTR1.2 mutant transporter with a large deletion of the last

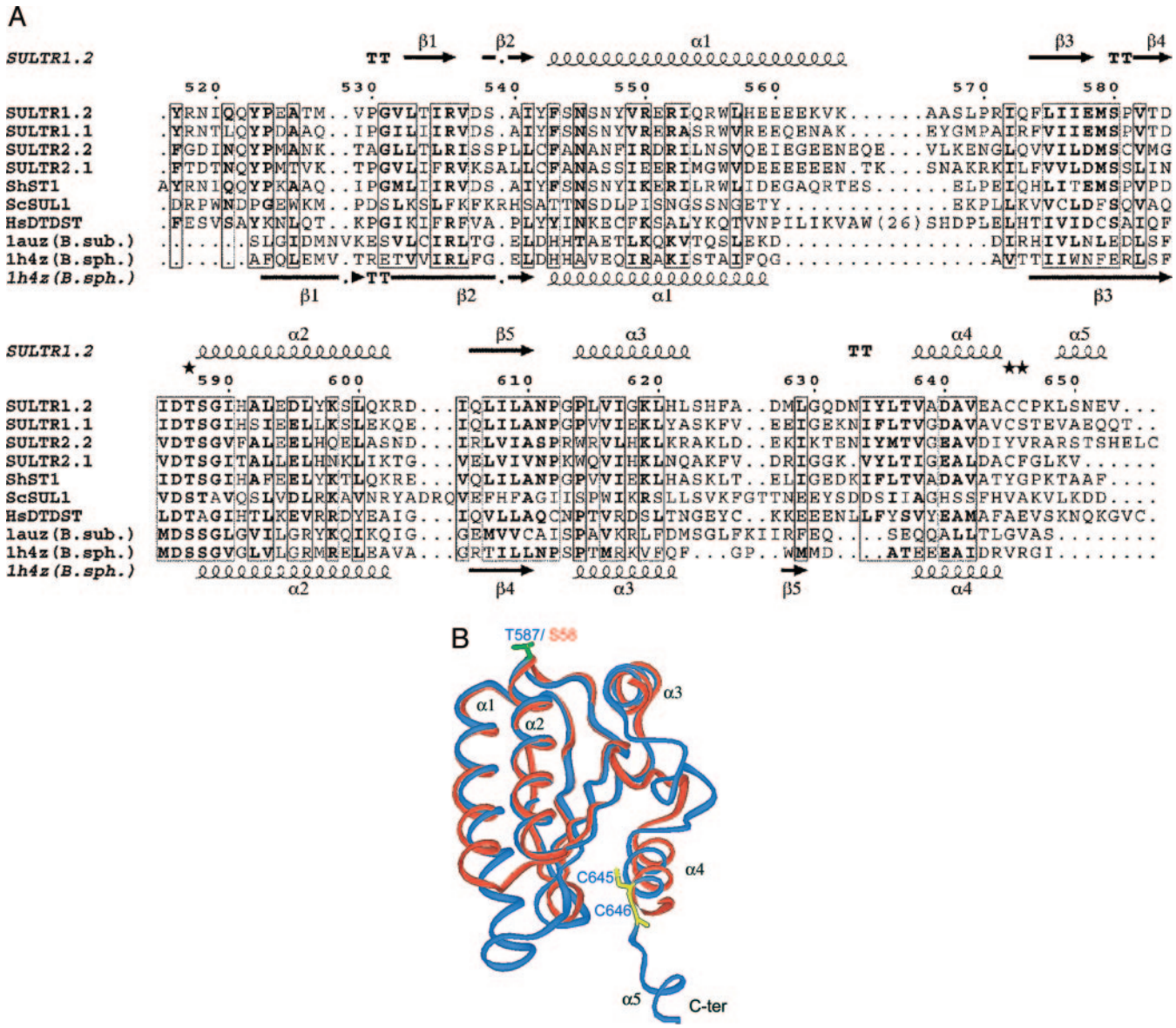

FIG. 1. **Modeling of the three-dimensional structure of the C-terminal SULTR1.2 STAS domain.** *A*, multiple protein sequence alignment of the STAS domains of different sulfate transporters including SULTR1.2 and of two SpoIIAA proteins. The alignment was refined manually from pairwise alignment obtained from our meta-server (18). The SpoIIAA proteins from *B. subtilis* (*B. sub.*) and from *B. sphaericus* (*B. sph.*) are represented by their PDB (www.rcsb.org/pdb) structure codes 1AUZ and 1H4Z, respectively. SWISSPROT accession numbers of the *A. thaliana* SULTR1.1, SULTR1.2, SULTR2.1, SULTR2.2, *S. hamata* ShST1, *Homo sapiens* DTDST, and *S. cerevisiae* SUL1 sulfate transporters are Q9SAY1, Q9MAX3, O04722, P92946, P53391, P50443, and P38359, respectively. Sequence alignment, drawing, and secondary structure assignment for the crystal structure PDB 1AUZ (21) and PDB 1H4Z (22) were performed using ESPRIPT (41). The *numbers above* the *sequence alignments* relate to the position of the corresponding amino acids in the *Arabidopsis* SULTR1.2 sequence. The *stars* indicate the amino acids that were changed in the site-directed mutagenesis experiments. *B*, three-dimensional model of the SULTR1.2 STAS domain. The crystal structure PDB 1H4Z and the deduced model of the SULTR1.2 STAS domain are shown in *red* and *blue ribbons*, respectively. The side chains of Thr-587 (Ser-58 in PDB 1H4Z) are represented in *green* and of the two cysteines (Cys-645 and Cys-646) of the SULTR1.2 STAS domain are in *yellow*. α-Helices are *numbered* and labeled sequentially. β-Strands are not labeled for clarity. The C terminus of the peptide is labeled, whereas its N terminus is hidden (behind helix α2) by the core of the structure.

131 amino acids of the protein corresponding to the entire STAS domain was constructed. This mutant transporter was expressed in the *S. cerevisiae* YSD1 mutant (19), which is defective in its sulfate transport capacity and, thus, unable to grow in the presence of 100 μM sulfate as the sole sulfur source. Although expressing the SULTR1.2 wild-type transporter in YSD1 restored growth of YSD1 in the presence of 100 μM sulfate as the sole sulfur source, expressing the mutant transporter in YSD1 did not induce any visible growth of YSD1 (Fig. 2*A*). Measurements of [^{35}S]sulfate influx showed that the mutant transporter was also unable to transport sulfate (Fig. 2*B*). These data show that the STAS domain is necessary for sulfate uptake by SULTR1.2 in yeast.

Functional Importance of the Very C Terminus of the SULTR1.2 STAS Domain—Sequence comparison of the STAS domains of the *A. thaliana* sulfate transporters showed that 9 (of 12) of the STAS domains possess one cysteine residue at the position corresponding to SULTR1.2 Cys-645 (Fig. 1*A* and data not shown). Depending on the transporter considered, the common cysteine residue is located 6–49 amino acids from the C-terminal end of the protein. The sequence analysis showed that this cysteine differentiated the *Arabidopsis* sulfate transporters from other sulfate transporters as well as from the bacterial SpoIIAA proteins. The importance of the very C terminus of SULTR1.2 for the functionality of this transporter was thus assessed. Mutant SULTR1.2 transporters displaying

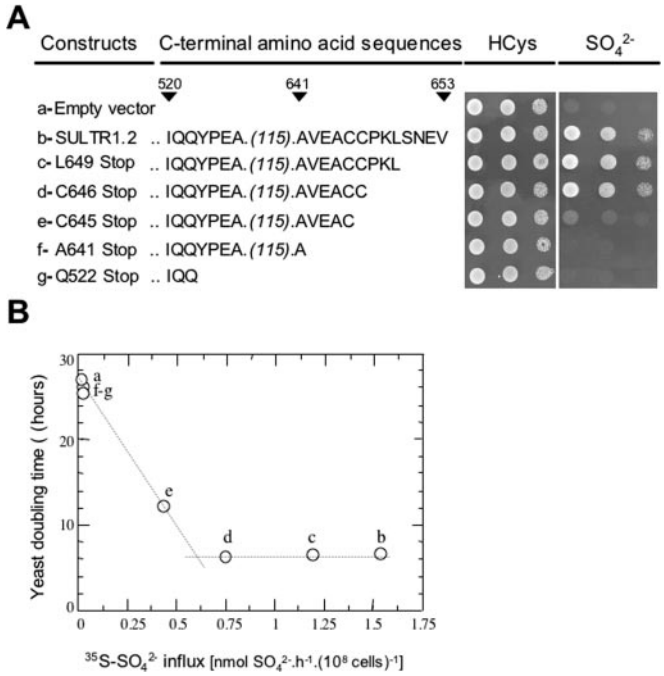

FIG. 2. **Growth phenotype and sulfate uptake capacity of the yeast YSD1 mutant expressing SULTR1.2 constructs displaying C-terminal deletions.** *A*, drop test analyses of the pYES2 vector empty (*a*) or containing serial deletions (*b–g*) of the C-terminal region of SULTR1.2 (as specified) were used to transform the yeast YSD1 mutant defective in its sulfate transport capacity. Yeast cells were grown in liquid synthetic media and adjusted to 1.0, 0.1, or 0.01 A_{600} unit. 30 μl of yeast suspensions were spotted onto agarose-selective synthetic minimal media supplemented with 0.1 mM homocysteine (*HCys*; *left panel*) or 0.1 mM sulfate (*right panel*) as the sole sulfur source. The picture was taken after 48 h of yeast growth at 30 °C. The *numbers above* the *sequence* relate to the position of the corresponding amino acids in the SULTR1.2 sequence. *B*, relationship between [^{35}S]sulfate short term influx measurements and the doubling time of the corresponding YSD1 yeast mutant transformed with the constructs (*a–g*) described in *panel A*. The *dotted lines* correspond to a least square adjustment. Sulfate uptake measurements are the means of two independent experiments.

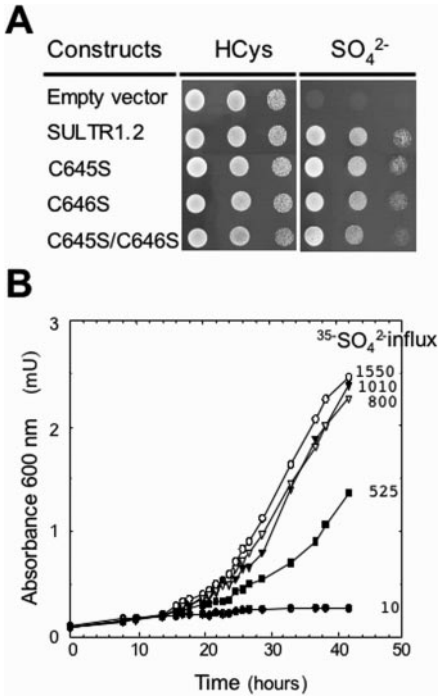

FIG. 3. **Growth and sulfate uptake capacity of the yeast YSD1 mutant expressing SULTR1.2 constructs obtained by site-directed mutagenesis of the C-terminal cysteine residues.** The yeast YSD1 mutant, which is defective in its sulfate transport capacity, contained the pYES2 empty vector (●), expressed the SULTR1.2 wild-type transporter (○), or expressed a mutant SULTR1.2 harboring the single C645S (▽) or C646S (▼) substitutions or the double C645S/C646S (■) substitution. *A*, drop test analysis was performed as described in Fig. 2*A*. *B*, yeast growth curves and [^{35}S]sulfate uptake capacity measurements (*numbers* on *curves*). Sulfate uptake results are expressed in pmol of SO_4^{2-}·h^{-1}·(10^8 cells)$^{-1}$ and are the means of two independent experiments.

serial C-terminal deletions were constructed and expressed in the YSD1 yeast mutant. As shown by [^{35}S]SO_4^{2-} influx measurements, deleting the last 4, 7, 8, or 12 amino acids of the SULTR1.2 C-terminal extension resulted in a corresponding 20, 50, 70, or 100% reduction in the ability of SULTR1.2 to transport sulfate (Fig. 2*B*). Therefore, the whole C terminus of SULTR1.2 is necessary to maintain the full transport capacity of this transporter. It is, however, noteworthy that the reduction of the transport capacity of SULTR1.2 did not always result in an alteration of the ability of SULTR1.2 to functionally complement the YSD1 mutant. Indeed, YSD1-expressing SULTR1.2 constructs bearing deletions of up to the last seven amino acids displayed comparable doubling time in liquid culture (Fig. 2*B*) and comparable growth in drop tests (Fig. 2*A*) to YSD1 expressing the wild-type SULTR1.2 transporter. In contrast, deleting the last 8 or 12 amino acids of SULTR1.2 severely reduced or blocked, respectively, the ability of SULTR1.2 to functionally complement the YSD1 mutant both in drop tests and in liquid culture. Thus, the ability of SULTR1.2 to complement the YSD1 mutant was altered when the capacity of SULTR1.2 to transport sulfate was lowered by more than 50% (Fig. 2*B*). This critical threshold was reached when eight or more amino acids were deleted from the end of SULTR1.2. Amazingly, the eighth and ninth amino acids from the end of the protein are the two cysteine residues that are specific to SULTR1·2. Altogether, the results of our deletion analysis show that the whole C terminus of SULTR1.2 is important to maintain the full capacity of SULTR1.2 to transport sulfate and that within this C terminus, the Cys-645 and Cys-646 seem to play a critical role to maintain the full functionality of SULTR1.2 in yeast.

Functional Role of Cysteine 645 and Cysteine 646 in Sulfate Transport by SULTR1.2—The implication of each of the two Cys-645 and Cys-646 residues in the functionality of SULTR1.2 was further investigated. Three mutant SULTR1.2 transporters were constructed by site-directed mutagenesis of the Cys-645 and Cys-646 residues. Two of these mutant transporters harbored the simple C645S and C646S substitutions, respectively, and the third one harbored the double C645S/C646S substitution. The C645S and C646S substitutions resulted in a 50 and 35% reduction of sulfate uptake, respectively, compared with the sulfate uptake by the wild-type SULTR1.2 (Fig. 3*B*). However, none of these substitutions induced an increase of the yeast doubling time in liquid culture (Fig. 3*B*). The double C645S/C646S substitution resulted in an additive effect of the two simple substitutions with respect to sulfate uptake (Fig. 3*B*). It also induced a ~60% increase in the yeast doubling time in liquid culture (Fig. 3*B*). These results show that each of the two Cys-645 and Cys-646 residues is important for optimum sulfate uptake by SULTR1.2. It is, however, noticeable that none of these residues is essential for the activity of SULTR1.2 since neither the simple C645S and C646S nor the double C645S/C646S substitutions completely abolished the ability of SULTR1.2 to complement the YSD1 mutant (Fig. 3*A*).

Functional Role of Thr-587 within the STAS Putative Phosphorylation Site—The three-dimensional modeling revealed that the DSSG phosphorylation site of SpoIIAA and its structural environment were well conserved in the SULTR1.2 STAS

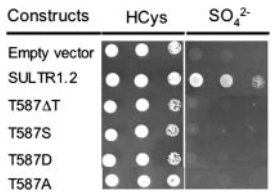

FIG. 4. **Growth phenotype of the yeast YSD1 mutant expressing SULTR1.2 constructs obtained by site-directed mutagenesis of Thr-587.** Drop test analysis was performed as described in Fig. 2*A*. The yeast YSD1 mutant, which is defective in its sulfate transport capacity, contained the pYES2 empty vector or expressed the SULTR1.2 wild-type transporter or SULTR1.2 mutants with either a deletion of the Thr-587 residue (T587ΔT) or harboring one of the substitutions, T587S, T587D, or T587A.

domain (Fig. 1*B*). In SpoIIAA, phosphorylation occurs on the first serine of the DSSG motif (9). The putative phosphorylation site of the SULTR1.2 STAS domain is DTSG; Thr-587 of SULTR1.2 corresponds to Ser-58 of SpoIIAA (Fig. 1*A*). Using site-directed mutagenesis, we constructed mutant SULTR1.2 transporters in which Thr-587 was deleted (T587ΔT) or was substituted either by serine (T587S), by alanine (T587A), or by aspartic acid (T587D). All the mutated transporters failed to restore growth of the YSD1 mutant in the presence of 100 μM sulfate as the sole sulfur source (Fig. 4). These results show that Thr-587 is critical for the function of SULTR1.2.

The Mutant SULTR1.2 Proteins Are Targeted to the Yeast Plasma Membrane—As shown above, all the SULTR1.2 transporters harboring a mutation in their STAS domain displayed a reduction, or even a lack of sulfate transport activity in yeast. This altered phenotype might have been the result of an erroneous targeting of the mutant transporters to the yeast plasma membrane, as has been suggested by Shibagaki and Grossman (15). We thus checked whether the presence of site-directed mutations could alter the targeting of the SULTR1.2 transporter to the yeast plasma membrane. To enable detection of the wild-type and mutant SULTR1.2 transporters by Western analysis, a FLAG® epitope was fused to the C termini of the wild-type transporter, of the mutant transporter displaying deletion of its last 12 amino acids, and of every mutant transporter displaying amino acid substitutions. When expressed in yeast, the flagged transporters induced the same phenotypes as the un-flagged ones (data not shown). Every truncated or mutated SULTR1.2 transporter appeared to be present in the plasma membrane-enriched fraction (Fig. 5). The mutant transporters were less abundant than the wild-type transporter in this fraction, suggesting that SULTR1.2 proteins altered in their capacity to transport sulfate are less stable and could be degraded more easily than the wild-type protein. A similar result has been observed for deletions of the whole STAS domain of SULTR1.2 (15). However, no significant difference was recorded in the targeting to the plasma membrane between constructions that only reduced (C645S, C646S, C645S/C646S) or completely abolished sulfate transport (A641STOP, T587A, T587S, T587ΔT, T587D). The lack of functionality of these latter mutant transporters could then be ascribed to the loss of the transporters ability to transport sulfate and not to an incorrect targeting to the plasma membrane.

DISCUSSION

The presence of a STAS domain in the C-terminal region of the SLC26 sulfate transporter family in all organisms, prokaryotes and eukaryotes (8), prompted us to investigate the functional importance of the STAS domain for sulfate transport in plants. We showed that deleting the whole STAS domain resulted in a complete loss of function of the *A. thaliana*

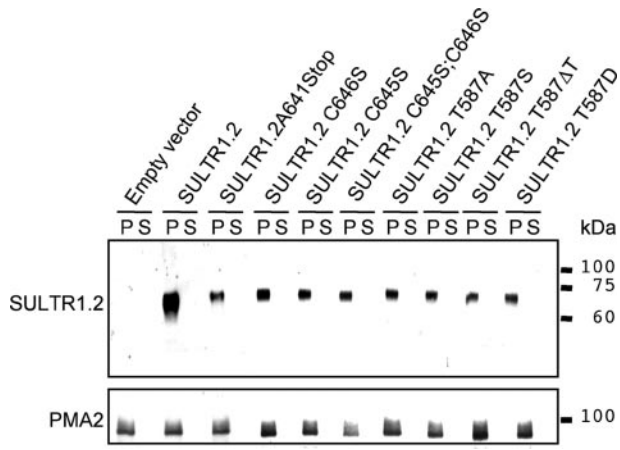

FIG. 5. **Mutant SULTR1.2 is addressed to the yeast plasma membrane.** Yeast strains containing the empty vector or expressing the FLAG-tagged wild-type SULTR1.2 protein or the different FLAG-tagged mutant transporters, as indicated on the *top*, were grown in synthetic B medium up to 0.2–0.4 A_{600} unit. The plasma membrane-enriched fraction was collected at the 37–53% interface of a sucrose gradient (25). Proteins (10 μg) from either the plasma membrane-enriched fraction (*P*) or the soluble fraction (*S*) were submitted to Western blot analysis. The anti-FLAG antibody and the anti-PMA2 antibody was used to reveal the SULTR1.2 protein and the yeast plasma membrane H^+-ATPase, respectively. Masses (in kDa) of the molecular markers are indicated on the *right*.

SULTR1.2 sulfate transporter and, thus, that the STAS domain is necessary for sulfate transport by SULTR1.2 as already recently found (15). Chernova *et al.* (30) similarly reported that the transport function of the human SLC26A3 Cl^--HCO_3^- exchanger requires the presence of its STAS domain. More generally, the crucial importance of the STAS domain for anion transport capacity is demonstrated by the fact that several point mutations in the STAS domain result in more or less severe alterations of the function of plant (this study) or animal transporters (12, 31–34). Although the STAS domain appears to be of crucial importance for the transport activity of the transporters, the precise role of this domain for sulfate transport is yet poorly understood.

Reviewing the characteristics of the transporters that possess a STAS domain is of little help to give an idea of the role of this domain. Indeed, the STAS domain is present in eukaryotic or prokaryotic sulfate transporters but not in all of them. It is also present in the 10 anion exchangers constituting the animal SLC26A family; these transporters exchange chloride for bicarbonate, hydroxyl, sulfate, formate, iodide, and/or oxalate (2). It is, however, remarkable that none of the sulfate or anion transporters that have been experimentally characterized as Na^+-dependent possess a STAS domain. It is also noticeable that the transport activity of most of the transporters that have a STAS domain (but not all of them) is regulated by pH (6, 30, 35). This raises the question of whether the STAS domain is associated with a particular mode of sulfate or anion transport.

Because the STAS domain is reminiscent of the bacterial SpoIIAA protein, clues to identify the functional role of the STAS domain could come from the current knowledge the *Bacillus* protein, the biochemical function of which has been fairly well described (11, 36). However, one should proceed with great caution since the amino acid identity between the STAS domain and the SpoIIAA proteins is lower than 20%. A remarkable result of our analysis of the structural similarity between the SULTR1.2 STAS domain and the bacterial SpoIIAA protein is that although these two proteins show only 17% of amino acid identity, their three-dimensional structures are similar (Fig. 1). Great confidence can be placed in this modeling result since the threading

scores are very high. Our comparative modeling showed that the highest identity between the STAS domain and SpoIIAA lies in the core domain of these peptides and also in the two regions that are crucial for SpoIIAA activity (37), the phosphorylation site and the protein-protein interaction region. This marked three-dimensional similarity strongly suggests that the study of the role of the STAS domain has to benefit from the knowledge available on SpoIIAA. We exploited the modeling work to guide our experimental mutagenesis work.

The deletion of the whole STAS domain abolished the transport of sulfate in the yeast mutant, which is in agreement with the recent study of Shibagaki and Grossman (15). We then set up a more detailed analysis of the effect of small deletions or site-directed mutagenesis within the STAS domain that alter or suppress the activity of this sulfate transporter. Serial deletions of the 12 C-terminal amino acids of SULTR1.2 decreased the sulfate transport capacity of the protein (Fig. 2*B*) without impairing its ability to be addressed to the plasma membrane (Fig. 5). Within this terminus region, the Cys-645 that is conserved in almost all *A. thaliana* sulfate transporters seemed to play, in conjunction with its adjacent Cys-646, a significant role in sulfate transport. However, we showed that these cysteines are not essential since a SULTR1.2 transporter mutant displaying a double substitution of these cysteines by serines is still able to transport sulfate (Fig. 3*B*). A functional assignment for these cysteines could be the formation of disulfide bonds. Because there are no other cysteine residues within the STAS domain, the disulfide bond would cross-link the STAS domain either to another domain of the transporter, maybe leading to di- or multimerization of the transporter, or to a partner protein. This latter hypothesis is in agreement with the role played by SpoIIAA (11) and the STAS domain of the human DRA sulfate transporter (14), which are both involved in protein-protein interaction with other partners. Such interpretations are compatible with our modeling since the cysteines are present in the α4-helix lying at the periphery of the STAS domain (Fig. 1*B*).

An alternative explanation of the role of this SULTR1.2 C terminus STAS domain is suggested by the presence of 6 hydrophobic residues between the last 10 amino acids (ACCPKLSNEV). The amphiphilic character of this C terminus, in conjunction with the fact that this region lies at the periphery of the STAS domain, suggests that this C terminus domain could dip into the membrane. Recently, the amphiphilic N and C termini of the yeast glycerol channel Fps1p, which were supposed to fold back into the membrane bilayer, were reported to restrict transport by this channel, thus regulating its activity (38, 39). The presence of a Cys-Cys sequence motif embedded in the amphiphilic C terminus sequence of SULTR1.2 reinforces the hypothesis that the C terminus of SULTR1.2 could dip into the membrane since these two cysteines might be post-translationally modified by prenylation, a mechanism assumed to enhance the abilities to associate with membranes by hydrophobic interactions (40).

In *B. subtilis*, SpoIIAA, which possesses the STAS signature, is a constituent of a regulatory network controlling the induction of sporulation (10). As already mentioned, the release of the sigma factor inducing sporulation is dependent from the phosphorylation status of SpoIIAA (9). Because of the three-dimensional folding identity at the phosphorylation site in both SpoIIAA and the STAS domain of SULTR1.2 (Fig. 1*B*), it seems reasonable to hypothesize that phosphorylation of the STAS domain is a key component of the activity of SULTR1.2. In plants, post-translational phosphorylation of plasma membrane proteins has been demonstrated for the H^+-ATPase (41) and an aquaporine (42) and recently for the low abundant nitrate transporter CHL1 (43). Between the STAS domains of the 12 *A. thaliana* sulfate transporters, 9 have a threonine, and 2 have a serine at the position corresponding to the phosphorylatable Ser-58 of SpoIIAA (Fig. 1 and data not shown). In SULTR1.2, Thr-587 is the residue that can be considered as the functional equivalent of the SpoIIAA Ser-58. The substitution of Thr-587 by a serine, a phosphorylatable residue in SULTR1.2 resulted in a loss of function of SULTR1.2 (Fig. 4). A comparable result was obtained for SpoIIAA; as a result of substitution of Ser-58 to threonine, sporulation was blocked, although the mutant S58T SpoIIAA was still able to interact with SpoIIAB (44). The phosphorylated serine and threonine residues have in some instances been functionally mimicked by the negatively charged amino acid aspartic acid (43, 45, 46). For SpoIIAA, a recent NMR study showed that the substitution of Ser-58 by aspartic acid induced structural perturbations of SpoIIAA (11), but the biochemical properties of the mutant protein were similar to those of SpoIIAA-phosphate (46). In the case of SULTR1.2, sulfate transport activity is not preserved when Thr-587 is changed for an aspartic acid residue (Fig. 4). This suggests either that aspartic acid could not mimic the putative phosphorylated Thr-587 or that Thr-587 is not phosphorylated. Finally, since deletion of Thr-587 (T587ΔT) or substitution of this residue by an aliphatic residue (alanine, T587A) did prevent SULTR1.2 from complementing the yeast mutant (Fig. 4), we concluded that a threonine is required at position 587 to sustain SULTR1.2 sulfate transport function when expressed in yeast.

The different mutated SULTR1.2 proteins were all correctly targeted to the plasma membrane, as revealed by their co-localization with the plasma membrane fraction marker H^+-ATPase (Fig. 5). This was equally true whatever the mutations resulted in a decrease in (C645S, C646S, C645S/C646S) or even a suppression of (A641STOP, T587A, T587S, T587D, T587ΔT) the sulfate transport capacity of SULTR1.2. This rules out the possibility that either the C-tail or the putative phosphorylation site (Thr-587) is directly or indirectly implied in the trafficking of SULTR1.2 in yeast. Our data are consistent with the fact that mutations within the linker region connecting the transmembrane region to the cytosolic STAS region more severely affect the association of SULTR1.2 with the plasma membrane than the deletion of the STAS domain itself (15). Our results clearly show that the differences observed in sulfate uptake capacity between yeast cells harboring constructs that can rescue or not rescue the mutant YSD1 phenotype are more likely explained by structural modifications that impair their ability to transport sulfate than by an improper cellular localization of the transporter.

In conclusion, the very high three-dimensional structural similarities between the STAS domain of SULTR1.2 and SpoIIAA and the results of our functional analysis revealed that the SULTR1.2 STAS domain could have, like SpoIIAA, a regulatory function. The recent finding that the STAS domain of the human chloride-bicarbonate exchanger DRA and the R domain of the cystic fibrosis transmembrane conductance regulator protein interact in epithelial cells (14) strengthen the idea that STAS domain could regulate anion transport via protein-protein interactions. Such interactions could depend on the phosphorylation status of the STAS domain and control plant sulfate transport activities.

Acknowledgments—We thank Dr. Marc Boutry (University of Louvain, Belgium) for the kind gift of *N. plumbaginifolia* PMA2 antibodies.

REFERENCES

1. Yoshimoto, N., Inoue, E., Saito, K., Yamaya, T., and Takahashi, H. (2003) *Plant Physiol.* **131,** 1511–1517
2. Mount, D. B., and Romero, M. F. (2004) *Pfluegers Arch.* **447,** 710–721
3. Hastbacka, J., de la Chapelle, A., Mahtani, M. M., Clines, G., Reeve-Daly,

M. P., Daly, M., Hamilton, B. A., Kusumi, K., Trivedi, B., Weaver, A., Coloma, A., Lovett, M., Buckler, A., Kaitila, I., and Lander, E. S. (1994) *Cell* **78,** 1073–1087
4. Hawkesford, M. J., Davidian, J. C., and Grignon, C. (1993) *Planta* **190,** 297–304
5. Smith, F. W., Ealing, P. M., Hawkesford, M. J., and Clarkson, D. T. (1995) *Proc. Natl. Acad. Sci. U. S. A.* **92,** 9373–9377
6. Smith, F. W., Hawkesford, M. J., Ealing, P. M., Clarkson, D. T., Vanden Berg, P. J., Belcher, A. R., and Warrilow, A. G. (1997) *Plant J.* **12,** 875–884
7. Markovich, D. (2001) *Physiol. Rev.* **4,** 1499–1533
8. Aravind, L., and Koonin, E. V. (2000) *Curr. Biol.* **10,** 53–55
9. Diederich, B., Wilkinson, J. F., Magnin, T., Najafi, M., Erringston, J., and Yudkin, M. D. (1994) *Genes Dev.* **8,** 2653–2663
10. Kroos, L., Zhang, B., Ichikawa, H., and Yu, Y. T. (1999) *Mol. Microbiol.* **31,** 1285–1294
11. Clarkson, J., Campbell, I. D., and Yudkin, M. D. (2003) *Biochem. J.* **372,** 113–119
12. Karniski, L. P. (2001) *Hum. Mol. Genet.* **10,** 1485–1490
13. Shelden, M. C., Loughlin, P., Tierney, M. L., and Howitt, S. M. (2001) *Biochem. J.* **356,** 589–594
14. Ko, S. B., Zeng, W., Dorwart, M. R., Luo, X., Kim, K. H., Millen, L., Goto, H., Naruse, S., Soyombo, A., Thomas, P. J., and Muallem, S. (2004) *Nat. Cell Biol.* **6,** 343–350
15. Shibagaki, N., and Grossman, A. R. (2004) *J. Biol. Chem.* **279,** 30791–30799
16. Maruyama-Nakashita, A., Inoue, E., Watanabe-Takahashi, A., Yamaya, T., and Takahashi, H. (2003) *Plant Physiol.* **132,** 597–605
17. Fizames, C., Munos, S., Cazettes, C., Nacry, P., Boucherez, J., Gaymard, F., Piquemal, D., Delorme, V., Commes, T., Doumas, P., Cooke, R., Marti, J., Sentenac, H., and Gojon, A. (2004) *Plant Physiol.* **134,** 67–80
18. Douguet, D., and Labesse, G. (2001) *Bioinformatics* **17,** 752–753
19. Sali, A., and Blundell, T. L. (1993) *J. Mol. Biol.* **234,** 779–815
20. Eisenberg, D., Luthy, R., and Bowie, J. U. (1997) *Methods Enzymol.* **277,** 396–404
21. Sippl, M. J. (1993) *Proteins* **17,** 355–362
22. Smith, F. W., Hawkesford, M. J., Prosser, I. M., and Clarkson, D. T. (1995) *Mol. Gen. Genet.* **247,** 709–715
23. Cherest, H., Davidian, J. C., Thomas, D., Benes, V., Ansorge, W., and Surdin-Kerjan, Y. (1997) *Genetics* **145,** 627–635
24. Vidmar, J. J., Tagmount, A., Cathala, N., Touraine, B., and Davidian, J. C. E. (2000) *FEBS Lett.* **475,** 65–69
25. Serrano, R. (1988) *Methods Enzymol.* **157,** 533–544
26. Schaffner, W., and Weissmann, C. (1973) *Anal. Biochem.* **56,** 502–514
27. Morsomme, P., Dambly, S., Maudoux, O., and Boutry, M. (1998) *J. Biol. Chem.* **273,** 34837–34842
28. Kovacs, H., Comfort, D., Lord, M., Campbell, I. D., and Yudkin, M. D. (1998) *Proc. Natl. Acad. Sci. U. S. A.* **95,** 5067–5071
29. Seavers, P. R., Lewis, R. J., Brannigan, J. A., Verschueren, K. H., Murshudov, G. N., and Wilkinson, A. J. (2001) *Structure* **9,** 605–614
30. Chernova, M. N., Jiang, L., Shmukler, B. E., Schweinfest, C. W., Blanco, P., Freedman, S. D., Stewart, A. K., and Alper, S. L. (2003) *J. Physiol.* **549,** 3–19
31. Hastbacka, J., Superti-Furga, A., Wilcox, W. R., Rimoin, D. L., Cohn, D. H., and Lander, E. S. (1996) *Am. J. Hum. Genet.* **58,** 255–262
32. Superti-Furga, A., Hastbacka, J., Wilcox, W. R., Cohn, D. H., van der Harten, H. J., Rossi, A., Blau, N., Rimoin, D. L., Steinmann, B., Lander, E. S., and Gitzelmann, R. (1996) *Nat. Genet.* **12,** 100–102
33. Kitamura, K., Takahashi, K., Noguchi, Y., Kuroishikawa, Y., Tamagawa, Y., Ishikawa, K., Ichimura, K., and Hagiwara, H. (2000) *Acta Otolaryngol.* **120,** 137–141
34. Lopez-Bigas, N., Melchionda, S., de Cid, R., Grifa, A., Zelante, L., Govea, N., Arbones, M. L., Gasparini, P., and Estivill, X. (2001) *Hum. Mutat.* **18,** 548
35. Xie, Q., Welch, R., Mercado, A., Romero, M. F., and Mount, D. B. (2002) *Am. J. Physiol. Renal Physiol.* **283,** 826–838
36. Bignell, D. R., Lau, L. H., Colvin, K. R., and Leskiw, B. K. (2003) *FEMS Microbiol. Lett.* **225,** 93–99
37. Clarkson, J., Campbell, I. D., and Yudkin, M. D. (2001) *J. Mol. Biol.* **314,** 359–364
38. Tamas, M. J., Karlgren, S., Bill, R. M., Hedfalk, K., Allegri, L., Ferreira, M., Thevelein, J. M., Rydstrom, J., Mullins, J. G., and Hohmann, S. (2003) *J. Biol. Chem.* **278,** 6337–6345
39. Hedfalk, K., Bill, R. M., Mullins, J. G., Karlgren, S., Filipsson, C., Bergstrom, J., Tamas, M. J., Rydstrom, J., and Hohmann, S. (2004) *J. Biol. Chem.* **279,** 14954–14960
40. Sinensky, M. (2000) *Biochim. Biophys. Acta* **1529,** 203–209
41. Maudoux, O., Batoko, H., Oecking, C., Gevaert, K., Vandekerckhove, J., Boutry, M., and Morsomme, P. (2000) *J. Biol. Chem.* **275,** 17762–17770
42. Johansson, I., Karlsson, M., Shukla, V. K., Chrispeels, M. J., Larsson, C., and Kjellbom, P. (1998) *Plant Cell* **10,** 451–459
43. Liu, K. H., and Tsay, Y. F. (2003) *EMBO J.* **22,** 1005–1013
44. Duncan, L., Alper, S., and Losick, R. (1996) *J. Mol. Biol.* **260,** 147–164
45. Wang, Y. H., Duff, S. M., Lepiniec, L., Cretin, C., Sarath, G., Condon, S. A., Vidal, J., Gadal, P., and Chollet, R. (1992) *J. Biol. Chem.* **267,** 16759–16762
46. Lord, M., Magnin, T., and Yudkin, M. D. (1996) *J. Bacteriol.* **178,** 6730–6735

Structural and Functional Analysis of the C-terminal STAS (Sulfate Transporter and Anti-sigma Antagonist) Domain of the *Arabidopsis thaliana* Sulfate Transporter SULTR1.2

Hatem Rouached, Pierre Berthomieu, Elie El Kassis, Nicole Cathala, Vincent Catherinot, Gilles Labesse, Jean-Claude Davidian and Pierre Fourcroy

J. Biol. Chem. 2005, 280:15976-15983.
doi: 10.1074/jbc.M501635200 originally published online February 16, 2005
